AD-A050 753 SYRACUSE UNIV N Y F/G 9/5
DESIGN OF SKEWED ISOPHASORS OF ELECTROMAGNETIC EMITTERS.(U)
DEC 77 T K SARKAR F30602-75-C-0121
UNCLASSIFIED RADC-TR-77-423 NL

| OF |
AD A050753

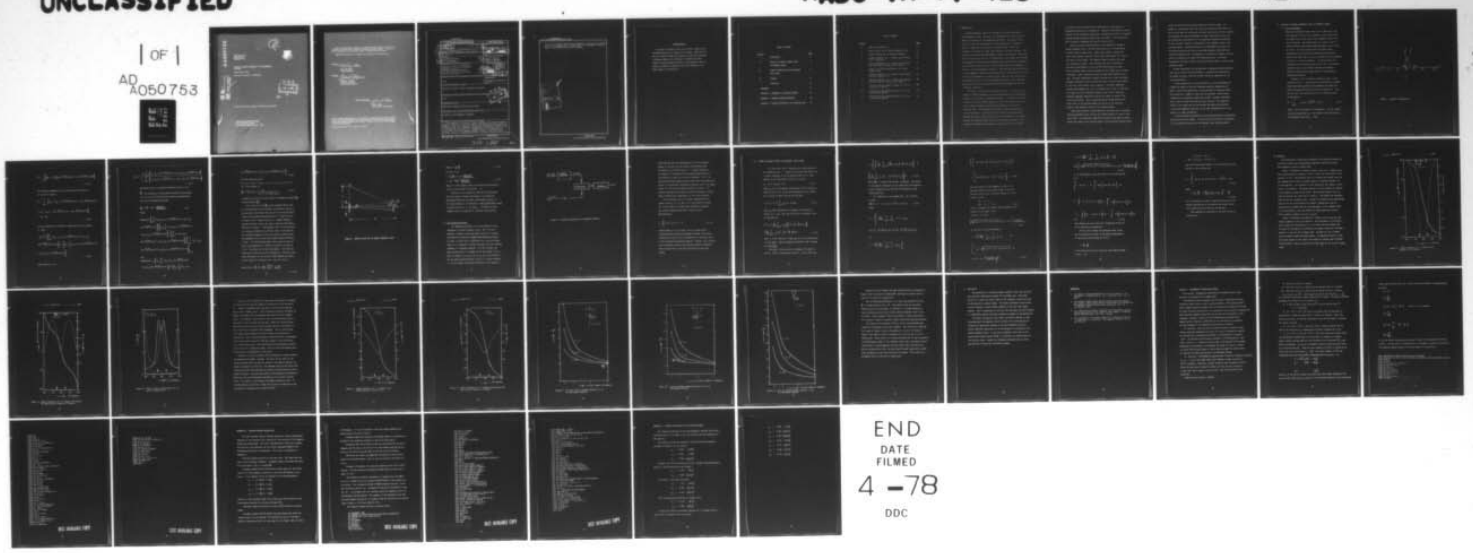

END
DATE FILMED
4 -78
DDC

RADC-TR-77-423
Phase Report
December 1977

DESIGN OF SKEWED ISOPHASORS OF ELECTROMAGNETIC EMITTERS

Tapan Kumar Sarkar

Rochester Institute of Technology

ROME AIR DEVELOPMENT CENTER
Air Force Systems Command
Griffiss Air Force Base, New York 13441

This report has been reviewed by the RADC Information Office (OI) and is releasable to the National Technical Information Service (NTIS). At NTIS it will be releasable to the general public, including foreign nations.

RADC-TR-77-423 has been reviewed and is approved for publication.

APPROVED: Paul Van Etten

PAUL VAN ETTEN
Project Engineer

APPROVED: Joseph L. Ryerson

JOSEPH L. RYERSON
Technical Director
Surveillance Division

FOR THE COMMANDER: John P. Huss

JOHN P. HUSS
Acting Chief, Plans Office

If your address has changed or if you wish to be removed from the RADC mailing list, or if the addressee is no longer employed by your organization, please notify RADC (OCTS) Griffiss AFB NY 13441. This will assist us in maintaining a current mailing list.

Do not return this copy. Retain or destroy.

UNCLASSIFIED

SECURITY CLASSIFICATION OF THIS PAGE (When Data Entered)

REPORT DOCUMENTATION PAGE

READ INSTRUCTIONS BEFORE COMPLETING FORM

1. REPORT NUMBER: RADC-TR-77-423	2. GOVT ACCESSION NO.
3. RECIPIENT'S CATALOG NUMBER	
4. TITLE (and Subtitle): DESIGN OF SKEWED ISOPHASORS OF ELECTROMAGNETIC EMITTERS.	5. TYPE OF REPORT & PERIOD COVERED: Phase Report Mar 77 - Sept 77
6. PERFORMING ORG. REPORT NUMBER: N/A	
7. AUTHOR(s): Tapan Kumar Sarkar	8. CONTRACT OR GRANT NUMBER(s): F30602-75-C-0121 new
9. PERFORMING ORGANIZATION NAME AND ADDRESS: Rochester Institute of Technology, Department of Electrical Engineering, Rochester NY 14623	10. PROGRAM ELEMENT, PROJECT, TASK AREA & WORK UNIT NUMBERS: 62702F 95670016 00
11. CONTROLLING OFFICE NAME AND ADDRESS: Rome Air Development Center (OCTS), Griffiss AFB NY 13441	12. REPORT DATE: Dec 77
	13. NUMBER OF PAGES: 45 (49 p.)
14. MONITORING AGENCY NAME & ADDRESS (if different from Controlling Office): Same	15. SECURITY CLASS. (of this report): UNCLASSIFIED
	15a. DECLASSIFICATION/DOWNGRADING SCHEDULE: N/A

16. DISTRIBUTION STATEMENT (of this Report)

Approved for public release, distribution unlimited.

17. DISTRIBUTION STATEMENT (of the abstract entered in Block 20, if different from Report)

Same

18. SUPPLEMENTARY NOTES

RADC Project Engineer: Paul Van Etten (OCTS)

19. KEY WORDS (Continue on reverse side if necessary and identify by block number)

Isophasors, Electromagnetic, Radiation

20. ABSTRACT (Continue on reverse side if necessary and identify by block number)

The magnitude of the slope of skewed isophasor lines from electromagnetic emitters is shown to be directly related to the physical distance between the geometric center of the spatially distributed electromagnetic emitters and the projected phase cebter obtained by extrapolation of the skewed isophasor lines. It is shown that the slope of the isophasor lines not only depends on the excitations of the electromagnetic emitters but also on the inter-emitter spacing. Finally, an optimization method is utilized to obtain the excitations

DD FORM 1 JAN 73 1473 EDITION OF 1 NOV 65 IS OBSOLETE

UNCLASSIFIED

SECURITY CLASSIFICATION OF THIS PAGE (When Data Entered)

339 600

for a set of spatially distributed electromagnetic emitters for a specified slope of the isophasor lines, a fixed number of electromagnetic emitters and for a given minimum inter-emitter spacing.

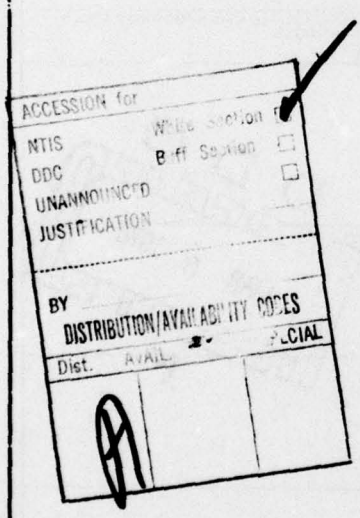

ACKNOWLEDGEMENT

The author is grateful to Mr. Paul Van Etten of RADC for his continued interest in all aspects of the problem. Thanks are also due to Dr. James E. Palmer for providing a stimulating environment at Rochester Institute of Technology for studying the myriad problem of skewed-isophasor synthesis of electromagnetic emitters. Finally, the author is indebted to Mrs. Nicole Bruening for her expert typing of the manuscript.

TABLE OF CONTENTS

LIST OF FIGURES

I. INTRODUCTION

An electromagnetic emitter is defined as a source which emits electromagnetic waves. The wave as it propagates out from the source display a variation of both amplitude and phase. The points on the wave which have the same phase in a given region may be thought of joined by imaginary lines, known as isophasor lines. These are analogous to contours on a map, which define a constant elevation. For a point source emitting electromagnetic waves, the isophasor lines would then form concentric circles. The objective of this report is to design electromagnetic emitters whose isophasor lines would not form concentric circles with the center of the circles being located at the geometric center of the electromagnetic emitters. This implies that such an array of electromagnetic emitters would produce over a certain angle in the far field an electromagnetic wave whose phase center may not coincide with the geometric center of the electromagnetic emitters. The projected phase center may even be outside the spatial distribution of the electromagnetic emitters.

The report is organized in various sections. In section II the design of skewed isophasor lines is presented when the electromagnetic emitters are excited by a band-limited signal. The analysis has been carried out in the frequency domain. Section III presents the analysis of skewed isophasor lines when the emitters are excited by arbitrary time. The development for this case has been presented in the time domain. In both sections II and III the relationship between the slope of the isophasor lines to the measure of closeness between the projected phase center and the geometric center of the spatially distributed electromagnetic emitters has been developed.

In section IV some representative computations are made using an optimization method due to Rosenbrock. Appendix A describes the salient features of the optimization procedure. Appendix B provides the computer program listing along with sample input and output. This program has been utilized in obtaining the results of section IV.

There are various applications of this principle of design of skewed isophasor lines. One such application is to the phenomenon of angle noise or angle glint. Angle noise causes a change with time in the apparent location of the target with respect to a reference point on the target. The apparent angular location may even fall outside the target. This principle may thus be applied in providing misinformation to the receiver monitoring the target. This is because target locating systems can be divided into two major categories: phase comparison systems and amplitude comparison systems. The phase comparison technique involves two or more receiving elements separated in space so that the phase of the received signal at the two or more points can be compared. The phase comparison systems then measures the tilt of the phase front since it indicates the target to be in a direction normal to the line of receiving elements alignment required to receive the signal in phase at the receiving structure. Thus a phase comparison system measures the phase front of the received signal and points to the direction normal to the isophasor lines of the received signal.

Amplitude comparison systems generally use some type of secondary receiving elements which focuses the received signal to a spot in the focal plane. All amplitude comparison systems by some means or other, locate the target as the pointing angle of the receiving elements which

center the spot from the received signal in the focal plane. For example, a conventional amplitude comparison monopulse radar split the spot in four parts by a multiport feed such that the spot can be centered by adjusting the receiving elements for equal amplitudes in each port. The significant characteristic of the amplitude comparison techniques is that the spot location is determined by the isophasor lines of the received signal. Centering the spot is accomplished by rotating the receiving structure such that the receiving elements align with the received isophasor lines. Consequently, in general any target locating device is essentially a phase front measuring device. From this measurement the device tries to project the phase center of the received isophasor lines.

Another application of the principle of designing skewed isophasor lines may be found in missile guidance. A missile may be guided by the skewed isophasor lines and thereby reduce the complexity of the tracking mechanism.

A third application of this principle is a very interesting one. Goldman has shown in his book "Frequency Analysis, Modulation and Noise", that by the application of the principle of stationary phase the location of a signal in time could be obtained. Under certain conditions the transmitted signal may be made to appear originating from a point in time other than its true location. This apparent origin of the signal may even be outside the spatial distribution of the electromagnetic emitters, as the time information may be converted to a range information.

A fourth possible application of this principle may be in Displaced Phase Center Antenna (DPCA). It may be possible this way to compensate for the deleterious effects of the airborne radar platform motion.

II. ANALYSIS OF SKEWED ISOPHASOR LINES IN FREQUENCY DOMAIN

2.1 For CW Waveforms

When the transmitted signal from a set of emitters is CW, the isophasor lines of such a signal is easy to visualize. The phase front in this case is the isophasor line of the set of emitters. The problem then is to select a set of emitters which would produce skewed isophasor lines in the far field. The tilt would be such that phase front measuring device looking at the waveform would project a phase center which may or may not coincide with the geometric location of the set of emitters. In this section a relationship is also derived relating the tilt of the skewed isophasor lines to the distance between the geometric center and the projected phase center of the spatially distributed emitters.

Consider a set of emitters situated on the x - axis as shown in Fig. 1. Each emitter is excited with a complex signal amplitude S_n (having both magnitude and phase) and they are separated from each other by a distance d. The electric far field pattern due to 2N + 1 emitters could be obtained as

$$\vec{E} = \sum_{n=-N}^{N} S_n \exp\left(\frac{j2\pi\, nd}{\lambda} \sin\theta\right) \qquad (2.1)$$

where λ is the wavelength of transmission. Let the complex excitation amplitudes S_n of the emitters have real parts a_n and imaginary parts as b_n. Then

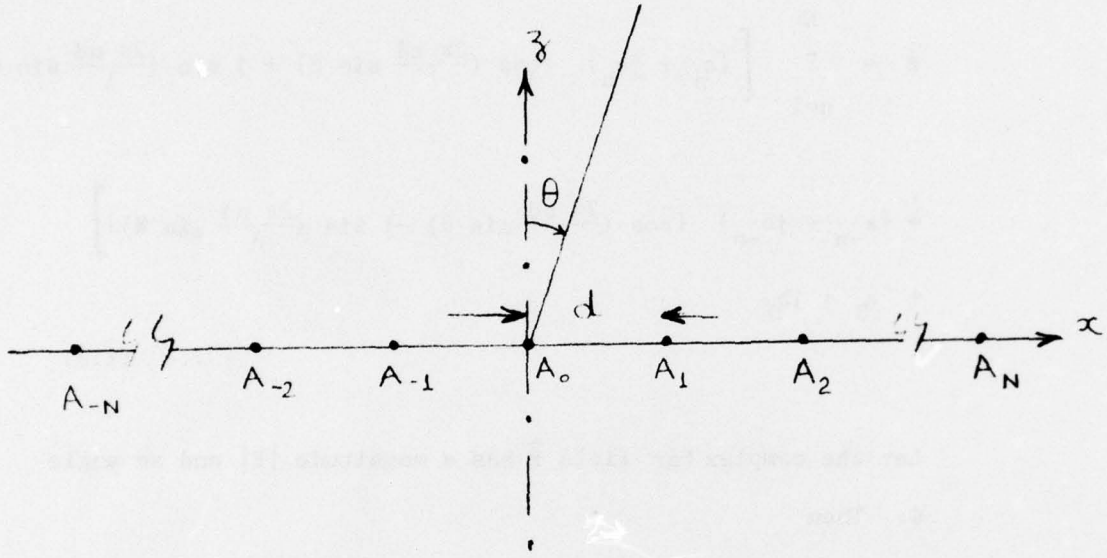

Figure 1. Emitter configuration

$$\vec{E} = \sum_{n=-N}^{N} \left[\{a_n + j\, b_n\} \{\cos\left(\frac{2\pi\, nd}{\lambda} \sin\theta\right) + j \sin\left(\frac{2\pi\, nd}{\lambda} \sin\theta\right)\} \right]$$

... (2.2)

By taking the summation now for only positive values of n in eq. (2.2) leads to

$$\vec{E} = \sum_{n=1}^{N} \left[\{a_n + jb_n\} \{\cos\left(\frac{2\pi\, nd}{\lambda} \sin\theta\right) + j \sin\left(\frac{2\pi\, nd}{\lambda} \sin\theta\right)\} \right.$$

$$\left. + \{a_{-n} + jb_{-n}\} \{\cos\left(\frac{2\pi\, nd}{\lambda} \sin\theta\right) - j \sin\left(\frac{2\pi\, nd}{\lambda} \sin\theta\right)\} \right]$$

$$+ a_0 + jb_0$$

... (2.3)

Let the complex far field $\vec{E}$ has a magnitude $|E|$ and an angle ψ. Then

$$|E|\, e^{j\psi} = \left[\sum_{n=1}^{N} \{(a_n + a_{-n}) \cos\left(\frac{2\pi\, nd}{\lambda} \sin\theta\right) + (b_{-n} - b_n) \sin\left(\frac{2\pi\, nd}{\lambda} \sin\theta\right)\} + a_0 \right] + j \left[b_0 + \sum_{n=1}^{N} \{(a_n - a_{-n}) \sin\left(\frac{2\pi\, nd}{\lambda} \sin\theta\right)\} \right.$$

$$\left. + (b_n + b_{-n}) \cos\left(\frac{2\pi\, nd}{\lambda} \sin\theta\right)\} \right]$$

... (2.4)

Hence from eq. (2.4)

$$\tan\psi = \frac{b_0 + \sum_{n=1}^{N}\left[(a_n - a_{-n})\sin\left(\frac{2\pi\, nd}{\lambda}\sin\theta\right) + (b_n + b_{-n})\cos\left(\frac{2\pi\, nd}{\lambda}\sin\theta\right)\right]}{a_0 + \sum_{n=1}^{N}\left[(a_n + a_{-n})\cos\left(\frac{2\pi\, nd}{\lambda}\sin\theta\right) + (b_{-n} - b_n)\sin\left(\frac{2\pi\, nd}{\lambda}\sin\theta\right)\right]} \quad \ldots (2.5)$$

The phase front in a particular direction θ has a tilt $\frac{d\psi}{d\theta}$. By carrying out the derivative operation with respect to θ in eq. (2.5) and after some algebric manipulations, the tilt is obtained as follows:

$$\frac{d\psi}{d\theta} = \frac{2\pi d}{\lambda}\cos\theta\ \frac{\text{Numerator}}{\text{Denominator}} \quad (2.6)$$

where,

$$\text{Numerator} = \left[\sum_{n=1}^{N} n\{(a_n - a_{-n})\cos\left(\frac{2\pi\, nd}{\lambda}\sin\theta\right) - (b_n + b_{-n})\sin\left(\frac{2\pi\, nd}{\lambda}\sin\theta\right)\}\right]\left[a_0 + \sum_{n=1}^{N}\{(a_n + a_{-n})\cos\left(\frac{2\pi\, nd}{\lambda}\sin\theta\right) - (b_n - b_{-n})\sin\left(\frac{2\pi\, nd}{\lambda}\sin\theta\right)\}\right] + \left[\sum_{n=1}^{N} n\{(a_n + a_{-n})\sin\left(\frac{2\pi\, nd}{\lambda}\sin\theta\right) + (b_n - b_{-n})\cos\left(\frac{2\pi\, nd}{\lambda}\sin\theta\right)\}\right]\left[\sum_{n=1}^{N}\{(a_n - a_{-n})\sin\left(\frac{2\pi\, nd}{\lambda}\sin\theta\right) + (b_n + b_{-n})\cos\left(\frac{2\pi\, nd}{\lambda}\sin\theta\right)\} + b_o\right] \quad \ldots (2.7)$$

and,

$$\text{Denominator} = \left[a_0 + \sum_{n=1}^{N}\{(a_n + a_{-n})\cos\left(\frac{2\pi\, nd}{\lambda}\sin\theta\right) - (b_n - b_{-n})\sin\left(\frac{2\pi\, nd}{\lambda}\sin\theta\right)\}\right]^2 + \left[b_0 + \sum_{n=1}^{N}\{(a_n - a_{-n})\right.$$

$$\sin\left(\frac{2\pi\, nd}{\lambda}\sin\theta\right) + (b_n + b_{-n})\cos\left(\frac{2\pi\, nd}{\lambda}\sin\theta\right)\Big\}\Big]^2 \qquad \ldots (2.8)$$

For the particular case,

$N=1,\ a_0 = 0,\ b_0 = 0,\ a_{+1} = 1,\ a_{-1} = a,\ b_{+1} = 0,\ b_{-1} = 0$

eq. (2.6) reduces to

$$\frac{d\psi}{d\theta} = \frac{2\pi\, d}{\lambda}\cos\theta\ \frac{1 - a^2}{1 + a^2 + 2a\left(\frac{4\pi\, d}{\lambda}\sin\theta\right)} \qquad \ldots (2.9)$$

Incidentally (2.9) is the same result as obtained by Meade [1] and Dean Howard [2].

Next, given the tilt $\frac{d\psi}{d\theta}$ of the isophasor lines, what is the separation distance between the geometric center of the spatially distributed emitters and the projected phase center from the phase measuring device. A typical set up is shown in Fig. 2 where the part of a skewed isophasor line PQ is shown to have come from a spatially distributed emitters of length A. The isophasor line is being observed at a distance R which is in the far field of the emitters. Two receiving elements P and Q are properly aligned along the isophasor line so that their measured phase difference is zero. So the projected phase center would be along TS which is perpendicular to PQ and is tilted at an angle β to OT. The object is to find the length L. Now the path difference between OP and OQ is $RQ(=\frac{\lambda}{2\pi}\, d\psi)$. Here $d\psi$ is the phase difference in the electric field between the points P and Q along the isophasor line. Also $PR = R\, d\theta$.

Hence $\tan\beta = \frac{OS}{OT} = \frac{L}{R} = \frac{RQ}{PR} = \frac{\frac{\lambda}{2\pi}\, d\psi}{R\, d\theta} = \frac{\lambda}{2\pi R}\frac{d\psi}{d\theta}$

$\ldots (2.10)$

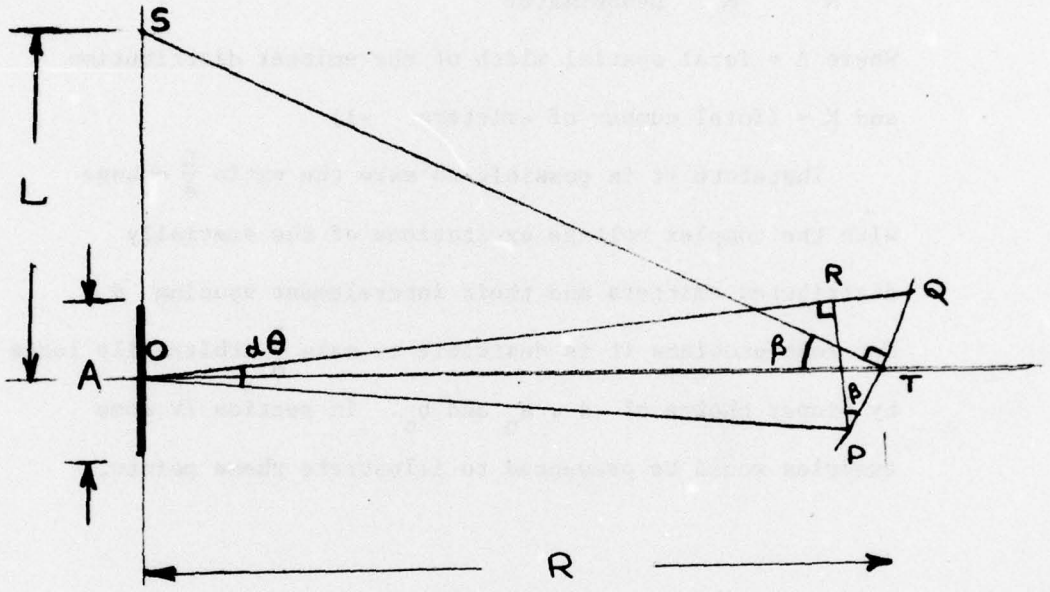

Figure 2. Spatial error due to skewed isophasor lines

Hence $L = \frac{\lambda}{2\pi} \frac{d\psi}{d\theta}$ ...(2.11)

So from (2.6)

$L = \frac{\lambda}{2\pi} \frac{d\psi}{d\theta} \; d \cos\theta \; \frac{\text{Numerator}}{\text{Denominator}}$

or $\frac{L}{A} = \frac{\cos\theta}{M} \; \frac{\text{Numerator}}{\text{Denominator}}$ ...(2.12)

Where A = Total spatial width of the emitter distribution

and M = (Total number of emitters -1)

Therefore it is possible to make the ratio $\frac{L}{A}$ change with the complex voltage excitations of the spatially distributed emitters and their interelement spacing d . For some problems it is desirable to make $\frac{L}{A}$ arbitrarily large by proper choice of d , a_n and b_n. In section IV some examples would be presented to illustrate these points.

2.2 For Wideband Waveforms:

For wideband waveforms, it is very difficult if not impossible to define isophasor lines. But it is still possible to define a projected phase center for a spatial distribution of emitters transmitting wideband waveforms. In order to obtain such a definition for a projected phase center it is necessary to define the model for the receiving elements of a wideband waveform. For this problem, the phase sensing device is assumed of the form shown in Fig. 3. Here two signals $x_1 (t_1,\theta_1)$ and $x_2 (t_1,\theta_2)$ are arriving at the two phase sensing devices A and B at a certain instance t. On one channel the Hilbert Transform of the signal is

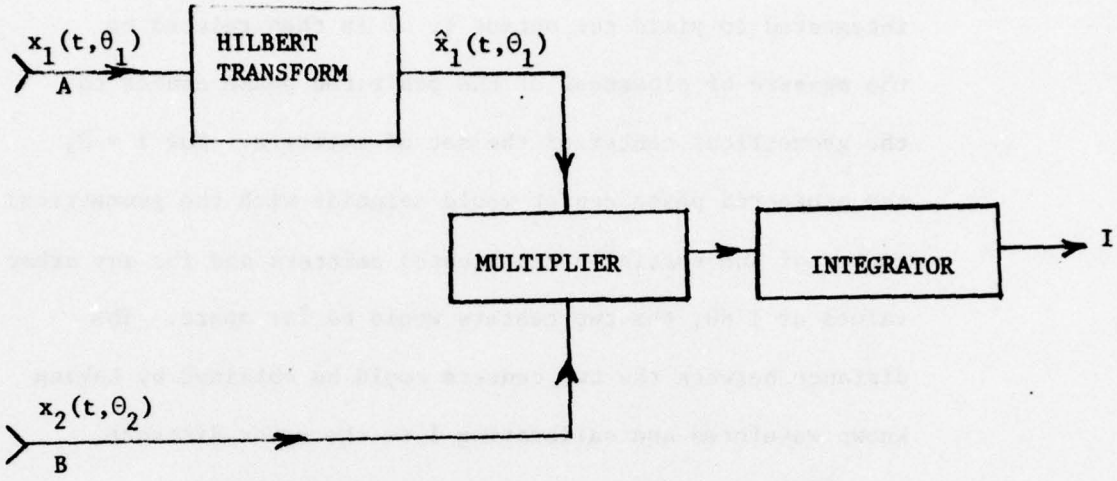

Figure 3. Receiver mechanism for a wideband waveform

performed and this is represented by $\hat{x}_1$ of the original signal x_1 and then the two signals are multiplied and integrated to yield the output I. I is then related to the measure of closeness of the projected phase center to the geometrical center of the set of emitters. For I = 0, the projected phase center would coincide with the geometrical center of the spatially distributed emitters and for any other values of I $\neq$0, the two centers would be far apart. The distance between the two centers could be obtained by taking known waveforms and calibrating I to the error distance.

For the special case of a signal originating from a single source x_1 (t, θ_1) and x_2 (t, θ_2) would be the same. For a real signal, the signal and its Hilbert Transform are always orthogonal and hence I would be zero. Mathematically,

$$I = \int_{-\infty}^{\infty} x(t)\, \hat{x}(t)\, dt = 0 \qquad \ldots(2.13)$$

always holds if x (t) is real. So for a single source transmitting any arbitrary wideband waveforms, this device would make no error at all in prediction of the phase center of the spatially distributed emitters. However, for a general case of multiple sources, the situation would be different. This is dealt with in the next section but in the time domain.

III. SKEWED ISOPHASOR DESIGN FOR ARBITRARY TIME SIGNALS

For this case a set of emitters are chosen similar to the diagram of Fig. 1. Instead of exciting each emitter by a single frequency as in the previous case of 2.1, each emitter is now excited by currents of the form

$$i_m (x,t) = A_m (x)\ f (t) \qquad \ldots(3.1)$$

where $A_m (x)$ is the spatial distribution of the current on emitter m and f (t) is the time dependence of the current. For an array of point sources one can write

$$i (x,t) = f (t) \sum_{m=-N}^{N} A_m (x)\ \delta(x-md) \qquad \ldots(3.2)$$

where $A_m (md)$ represents the strength of the discrete emitter at x = md. Now the far field at a distance R can be expressed as

$$\vec{E} (\theta,t) = \frac{\mu_0}{4\pi R} \sum_{m=-N}^{N} A_m \frac{\partial}{\partial t}\left[f\ (t- \frac{R}{c} + \frac{md}{c} \sin \theta)\right]$$

$$\triangleq \frac{\mu_0}{4\pi R} \sum_{m=-N}^{N} A_m\ F(t - \frac{R}{c} + \frac{md}{c} \sin \theta) \qquad \ldots(3.3)$$

where c is the velocity of light and μ_0 is the permittivity of free space. This is essentially equation (20) of Tseng and Cheng [3] .

The model of the receiver is assumed to be same as before. This is illustrated in Fig. 2. So for this case

$$I = \int_{T_1}^{T_2} \left[\frac{\mu_0}{4\pi R} \sum_{m=-N}^{N} A_m \mathcal{H}\{F\,(t - \frac{R}{c} + \frac{md}{c} \sin\theta_1)\} \right] \times$$

$$\left[\frac{\mu_0}{4\pi R} \sum_{k=-N}^{N} A_k \{F(t - \frac{R}{c} + \frac{kd}{c} \sin\theta_2)\} \right] dt \qquad \ldots(3.4)$$

where $\mathcal{H}\{\cdot\}$ denotes the Hilbert transform. The limits of integration correspond to the times when the integrator starts integrating (T_1) and when the integrator stops integrating (T_2).

For simplicity it is assumed that $f(t) = \sin \omega t$, so that

$$\mathcal{H}\{F\,(t)\} = \omega \cos\,(\omega t + 90^{\circ}) = -\omega \sin \omega t \qquad \ldots(3.5)$$

Hence,

$$I = \int_{T_1}^{T_2} (\frac{\mu_0}{4\pi R})^2 \sum_{m=-N}^{N} \sum_{k=-N}^{N} (-\omega^2)\; A_m A_k$$

$$\sin\,(\omega t - \frac{R}{c} + \frac{md}{c} \sin\theta_1) \cos\,(\omega t - \frac{R}{c} + \frac{kd}{c} \sin\theta_2)\, dt$$

or

$$I = -\frac{\omega^2}{2} (\frac{\mu_0}{4\pi R})^2 \sum_{m=-N}^{N} \sum_{k=-N}^{N} A_k A_m \left\{ \right.$$

$$\left[\int_{T_1}^{T_2} \sin\{ 2(\omega t - \frac{R}{c}) + \frac{d}{c} (m \sin \theta_1 + k \sin \theta_2) \right] dt$$

$$+ \int_{T_1}^{T_2} \left[\sin\{ \frac{d}{c}(m \sin \theta_1 - k \sin \theta_2)\} \right] dt \Bigg\} \quad \ldots \quad (3.6)$$

Since the purpose of the integrator in Fig. 2 is a smoothing operation, the average value of the first integral would be zero as the time average of a "sin" function is zero.

Let $\theta_2 = \theta$

and $\theta_1 = \theta + \Delta\theta$ ...(3.7)

where $\Delta\theta$ represent the azimuth angle subtended by the receiver at the origin. Then

$m \sin \theta_1 - k \sin \theta_2 =$

$$\left[\sqrt{(m \cos \Delta\theta - k)^2 + (m \sin \Delta\theta)^2} \right] \sin\left\{ \theta + \tan^{-1} \left\{ \frac{m \sin \Delta\theta}{m \cos \Delta\theta - k} \right\} \right\} \quad \ldots (3.8)$$

So the error I can be expressed as

$$I = -\frac{\omega^2}{2} \left(\frac{\mu_0}{4\pi R}\right)^2 \sum_{m=-N}^{N} \sum_{k=-N}^{N} A_k A_m \times$$

$$\int_{T_1}^{T_2} \sin \left[\sqrt{(m \cos \Delta\theta - k)^2 + (m \sin \Delta\theta)^2} \, \frac{d}{c} \right] \times$$

$$\sin \left\{ \theta + \tan^{-1} \left\{ \frac{m \sin \Delta\theta}{m \cos \Delta\theta - k} \right\} \right\} dt \quad \ldots (3.9)$$

$$I = -1/2 \left(\frac{\omega\mu_0}{4\pi R}\right)^2 \sum_{m=-N}^{N} \sum_{k=-N}^{N} A_k A_m \left(T_2 - T_1\right)$$

$$\sin\left[\frac{d}{c}\sqrt{(m\cos\Delta\theta - k)^2 + (m\sin\Delta\theta)^2}\,\sin\{\theta + \tan^{-1}\left(\frac{m\sin\Delta\theta}{m\cos\Delta\theta - k}\right)\right] \quad \ldots(3.10)$$

It is interesting to note that since I is an odd function of θ,

$$\int_0^{2\pi} I(\theta)\,d\theta = A\int_0^{2\pi} \sin\left[z\sin(\theta+\psi)\right]d\theta$$

$$= A\int_0^{\pi} \sin\left[z\sin(\theta+\psi)\right]d\theta + \int_{\pi}^{2\pi} \sin\left[z\sin(\theta+\psi)\right]d\theta$$

$$= A\int_0^{\pi} \left[\sin\; z\sin(\theta+\psi)\right]d\theta - \int_0^{\pi} \sin\left[z\sin(\theta+\psi)\right]d\theta$$

$$=0 \quad \ldots(3.11)$$

This implies that the total error integrated around the set of emitters is always zero.

Now the error between the projected phase center and the geometrical center of the spatial distribution of apertures would be given by (2.11).

$$L = \frac{\lambda}{2\pi}\,\frac{d\psi}{d\theta}$$

So the objective now is to find the relationship between I and ψ. Let

$$x_1 (t_1, \theta_1) = \sin \omega t$$

and $$x_2 (t_1, \theta_2) = \sin (\omega t + \psi)$$

then from a derivation similar to that presented in this section it can be shown that

$$I = \int_{T_1}^{T_2} \cos \omega t \ \sin (\omega t + \psi)\, dt = \frac{T_2 - T_1}{2} \sin \psi \qquad \ldots(3.12)$$

Hence

$$L = \frac{\lambda}{2\pi} \frac{d\psi}{d\theta} = \frac{\lambda}{\pi} \left\{ \frac{1}{(T_2 - T_1)^2 - 4I^2} \right\}^{\frac{1}{2}} \frac{dI}{d\theta} \qquad \ldots(3.13)$$

So it is possible to make L larger than the half of the spatial distribution of the emitters by proper choice of the amplitude coefficient of the emitters.

Some examples are presented in the next section to illustrate it.

IV. EXAMPLES

The mathematical formulations presented in the previous sections is utilized to obtain some representative numerical values for various electromagnetic emitter configuration.

Figure 4 represents the skewed isophasor lines of a 3 element array. The spacing between the elements is 1.5λ so that the total width of the aperture is 3.0λ. The objective then is to obtain the largest slope for the isophasor lines within an angle window of 10 degrees (between 175 and 185 degrees). The variables in this problem are the complex excitations of the elements. The phase reference for this diagram is referred to the geometric center of the array. The optimized phase of the far field is shown by the solid line in Figure 4. The dashed line represent the gain for the 3 element array. The gain is defined as the logarithimic ratio of the far field between the present 3 element array and an omnidirectional element fed with the same power as the 3 element array. It is interesting to note that within the angle window the electric field intensity remains relatively constant.

Figure 5 represents the optimized 2 element array having the same aperture length of 3.0λ as in Figure 4. This represents the optimized case of Meade [1] and Howard [2]. It is clear from this diagram that the slope of the phase of the E-field is no longer linear over the angle window as it was for the 3 element case. The gain for the 3 element case was higher outside the angle window. An important feature is that the linear portion of the slope of the phase is situated near a minimum field intensity. Figure 6 presents the slopes $(\frac{2L}{A})$ for the 2 and 3 element cases.

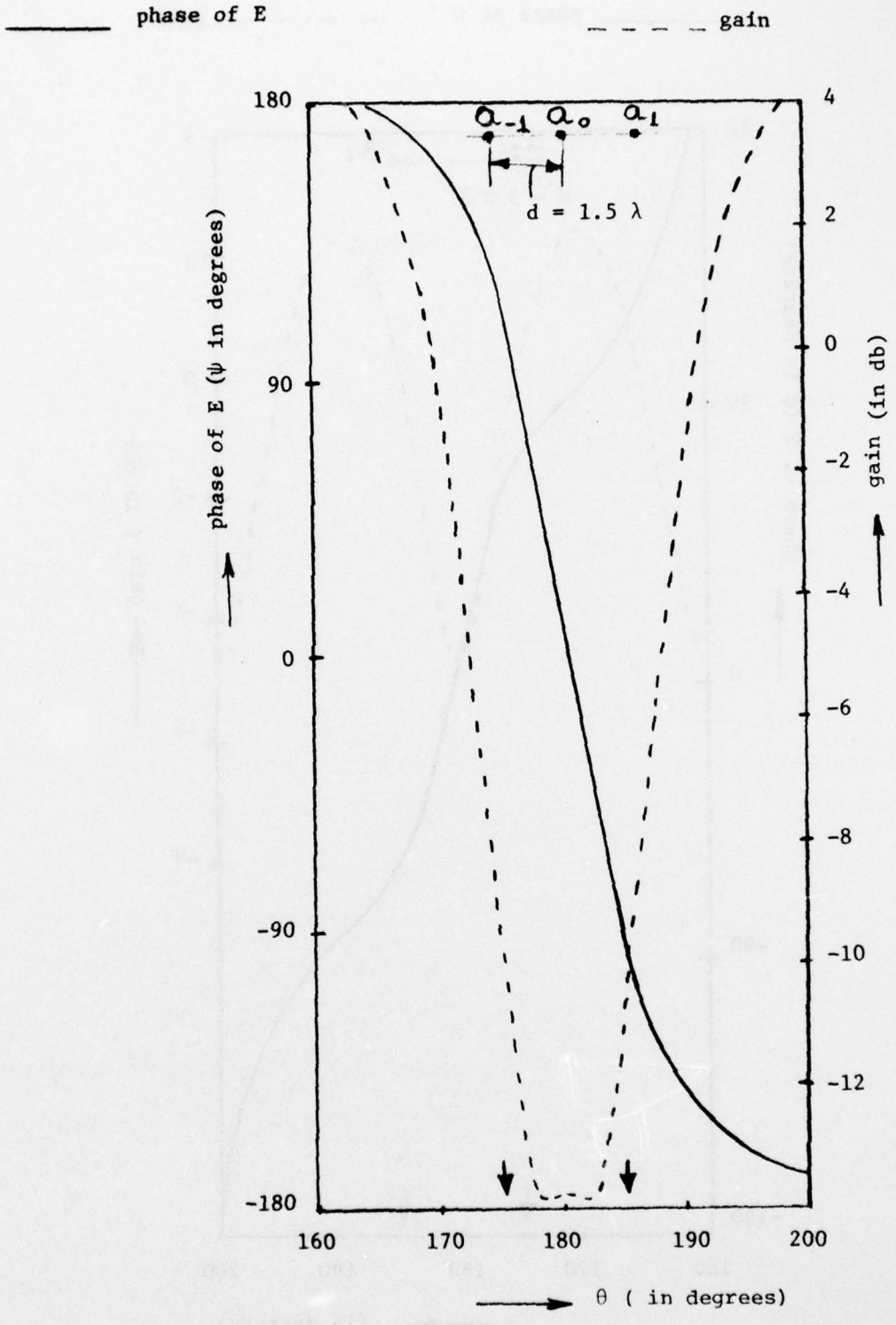

Figure 4: Skewed isophasors of a 3 element array having a 3.0 λ aperture

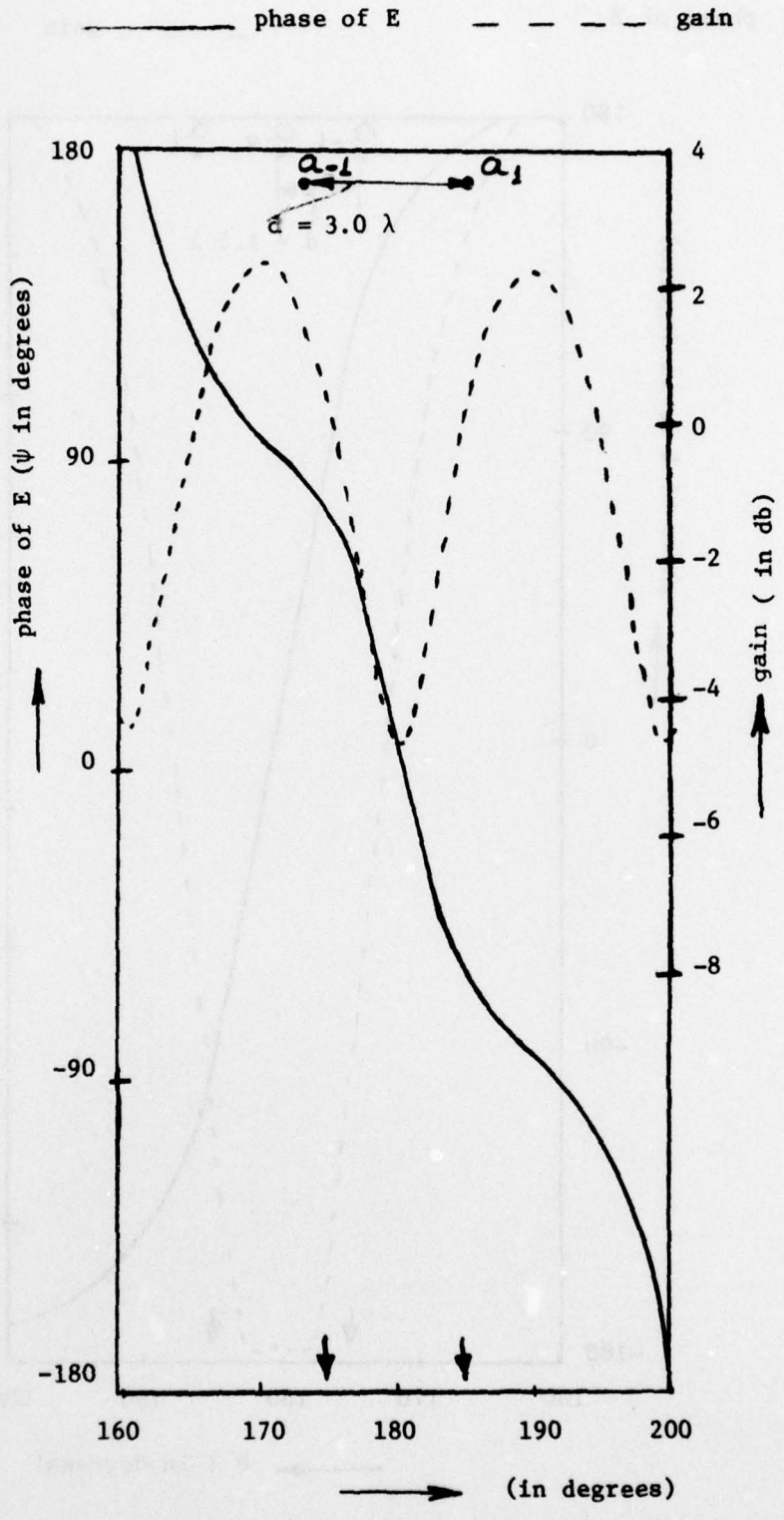

Figure 5: Skewed isophasors of a 2 element array having the same aperture length as of Figure 4.

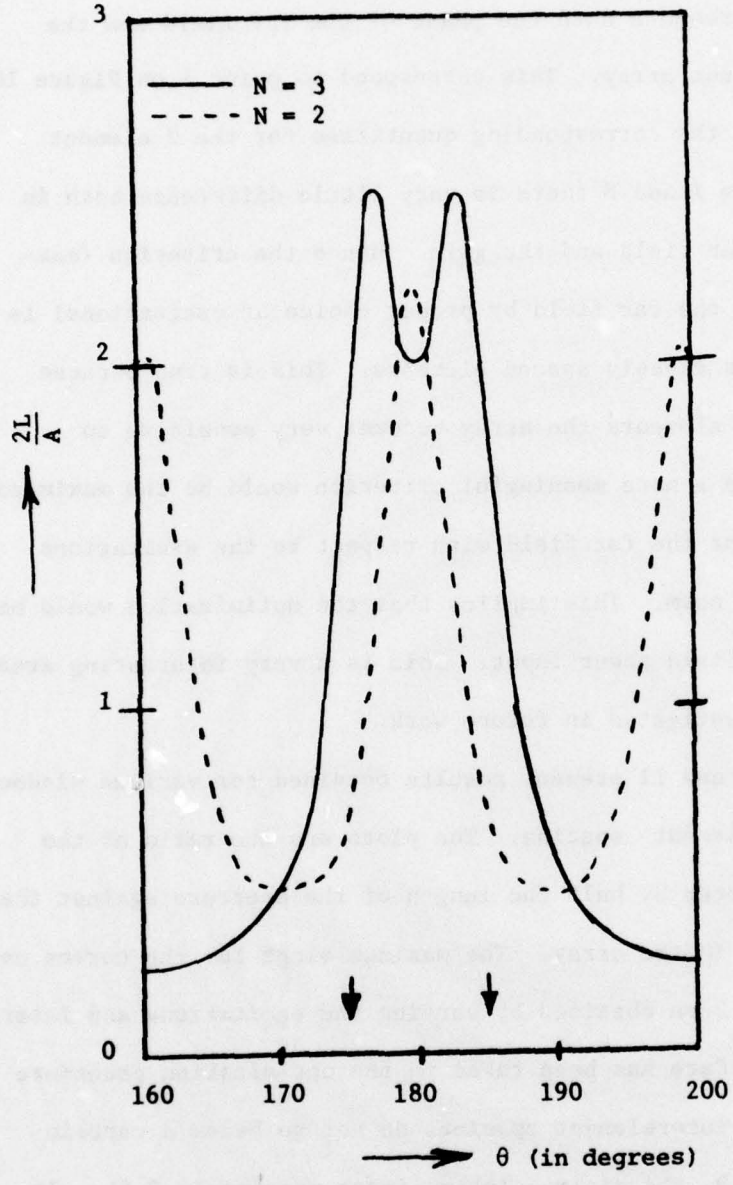

Figure 6: Slope of the far field phase for a 2 and a 3 element array

Figures 7 and 8 represent the same cases as presented in Figures 4-6 except now the aperture length is restricted to 0.6λ instead of 3λ. Figure 7 represents both the phase of the far field and the gain of the 3 element array. This correspond to point A on Figure 10. Figure 8 represent the corresponding quantities for the 2 element array. For Figures 7 and 8 there is very little difference both in the phase of the far field and the gain. Hence the criterion (maximize the slope of the far field by proper choice of excitations) is not a valid one for closely spaced elements. This is true because for closely spaced elements the array becomes very sensitive to excitations. Hence a more meaningful criterion would be the maximization of the slope of the far field with respect to the excitations for a fixed source norm. This implies that the optimization would be carried out for a fixed power input. This is a very interesting area which would be investigated in future work.

Figures 9, 10 and 11 present results obtained for various windows and minimum interelement spacing. The plots are the ratio of the projected phase center by half the length of the aperture against the number of elements in the array. The maximum slope for the curves over a given window has been obtained by varying the excitations and interelement spacings. Care has been taken in the optimization procedure to make sure that the interelement spacings do not go below a certain value. For Figure 9, the minimum interelement spacing is 0.5λ. It is interesting to note that a large ratio $\frac{L}{A}$ could be achieved for the same number of elements over a smaller window.

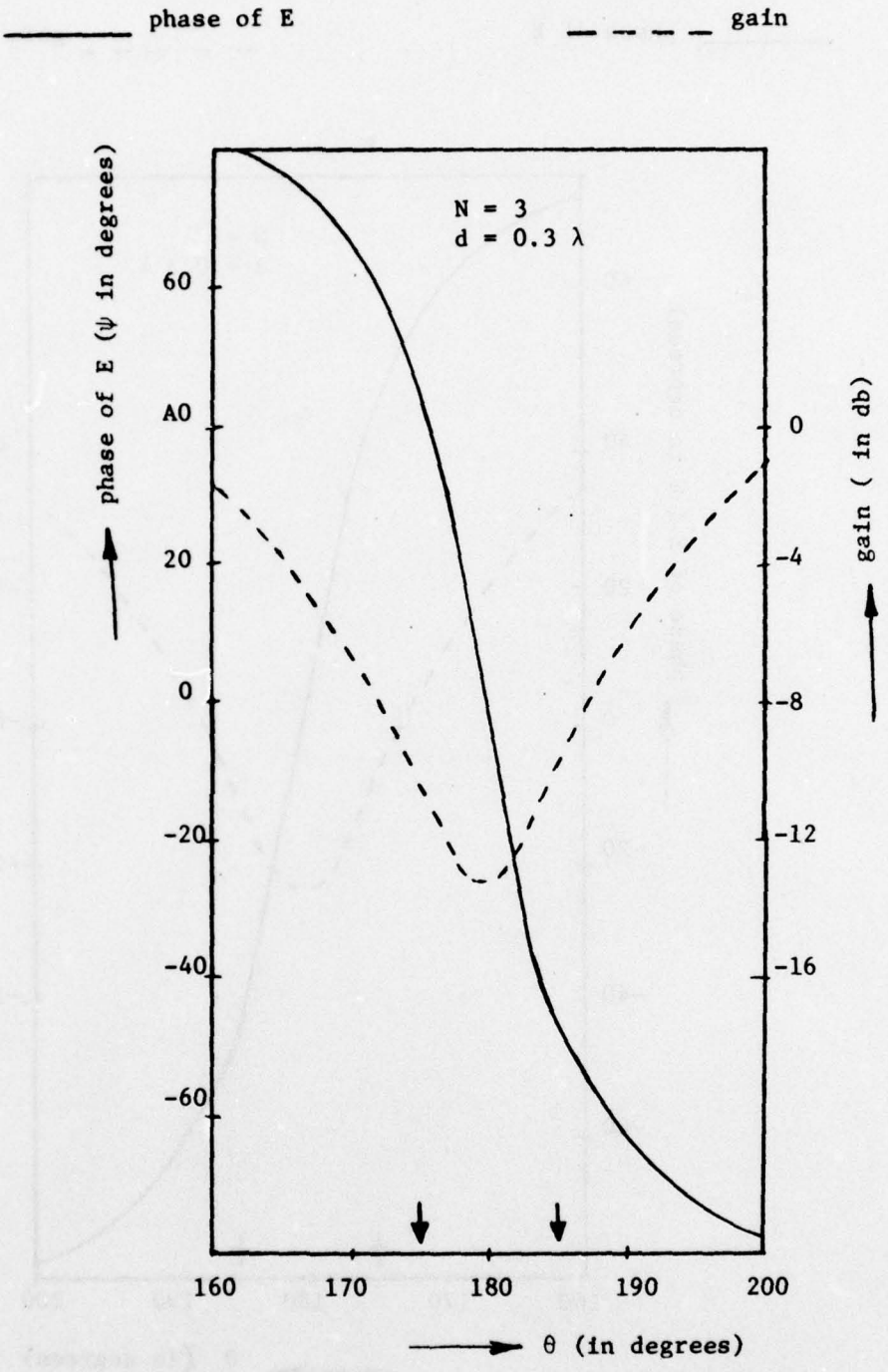

Figure 7: Skewed isophasors of a 3 element array having aperture length of 0.6 λ

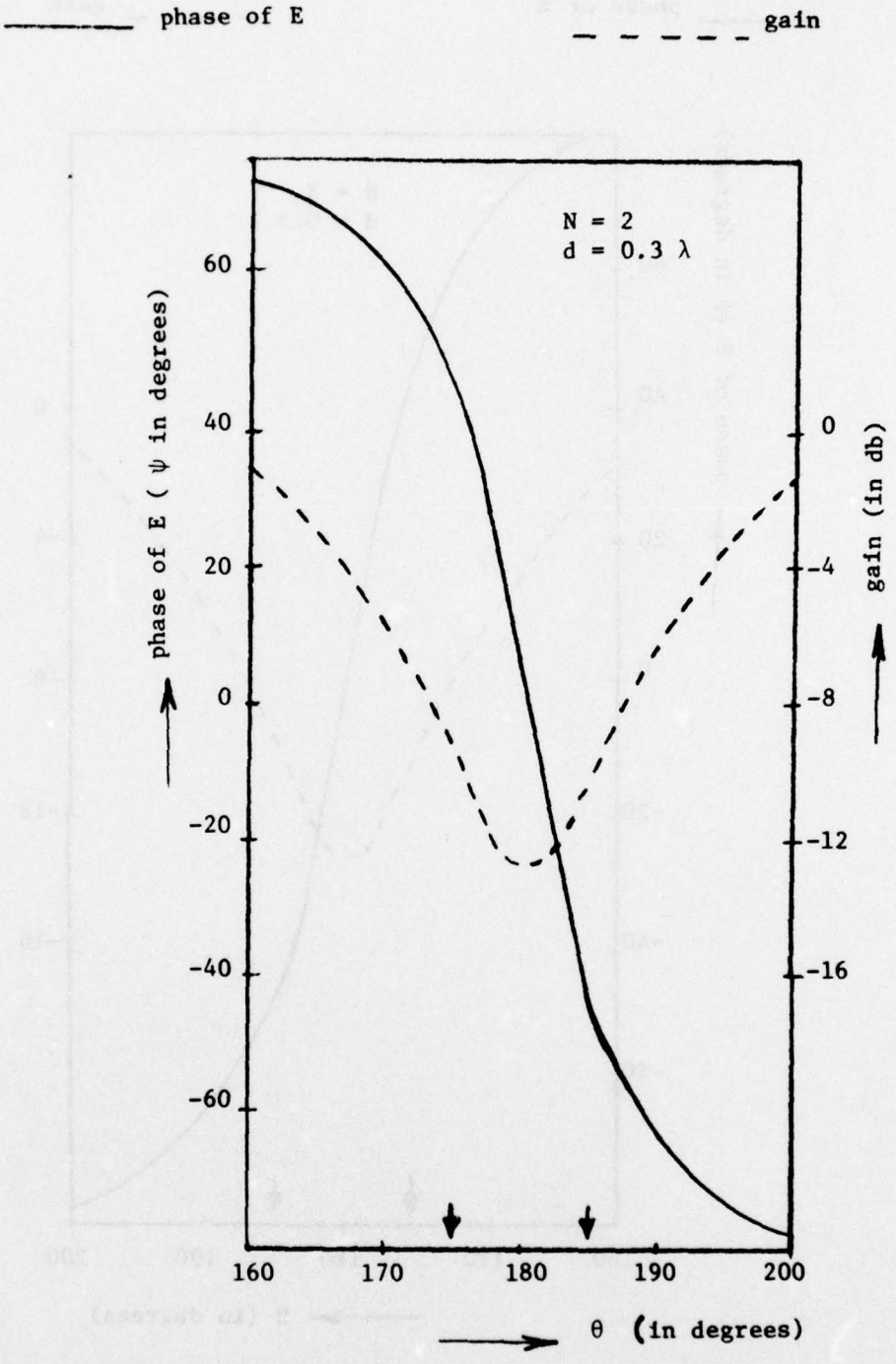

Figure 8: Skewed isophasors of a 2 element array having the same aperture length as of Figure 7

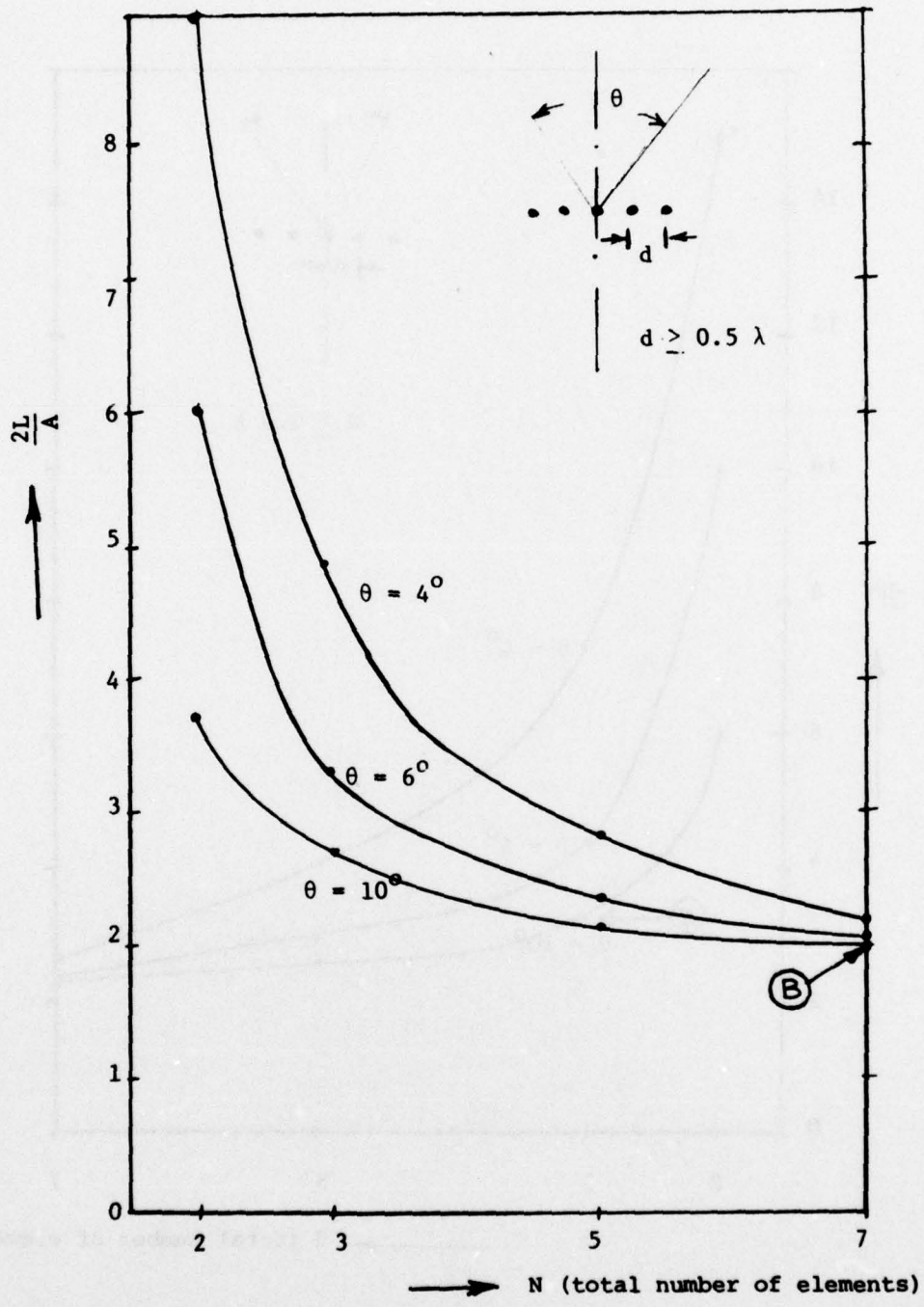

Figure 9: 2L/A for various elements having 0.5 λ as an interelement spacing

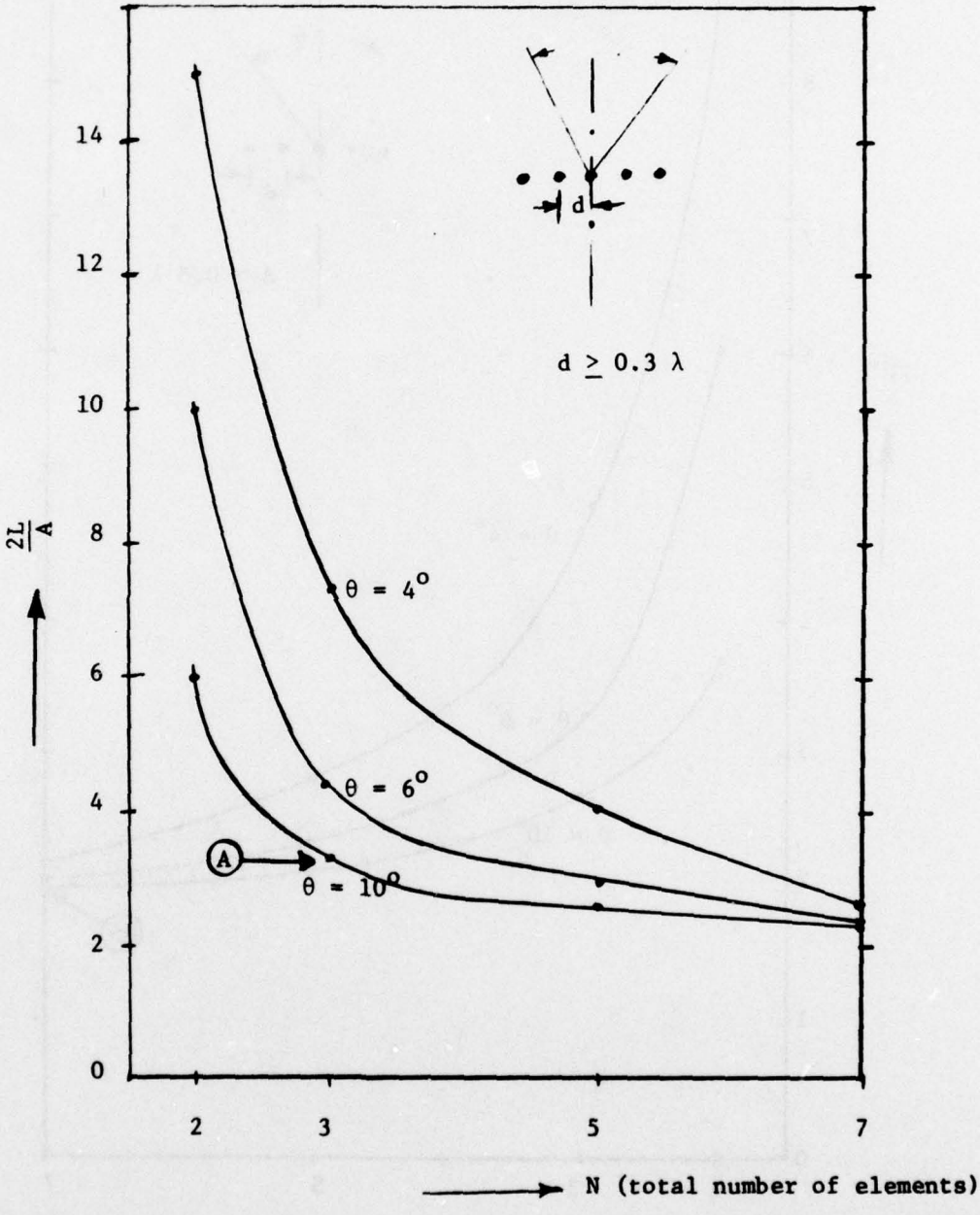

Figure 10: 2L/A for various elements having 0.3 λ as an interelement spacing

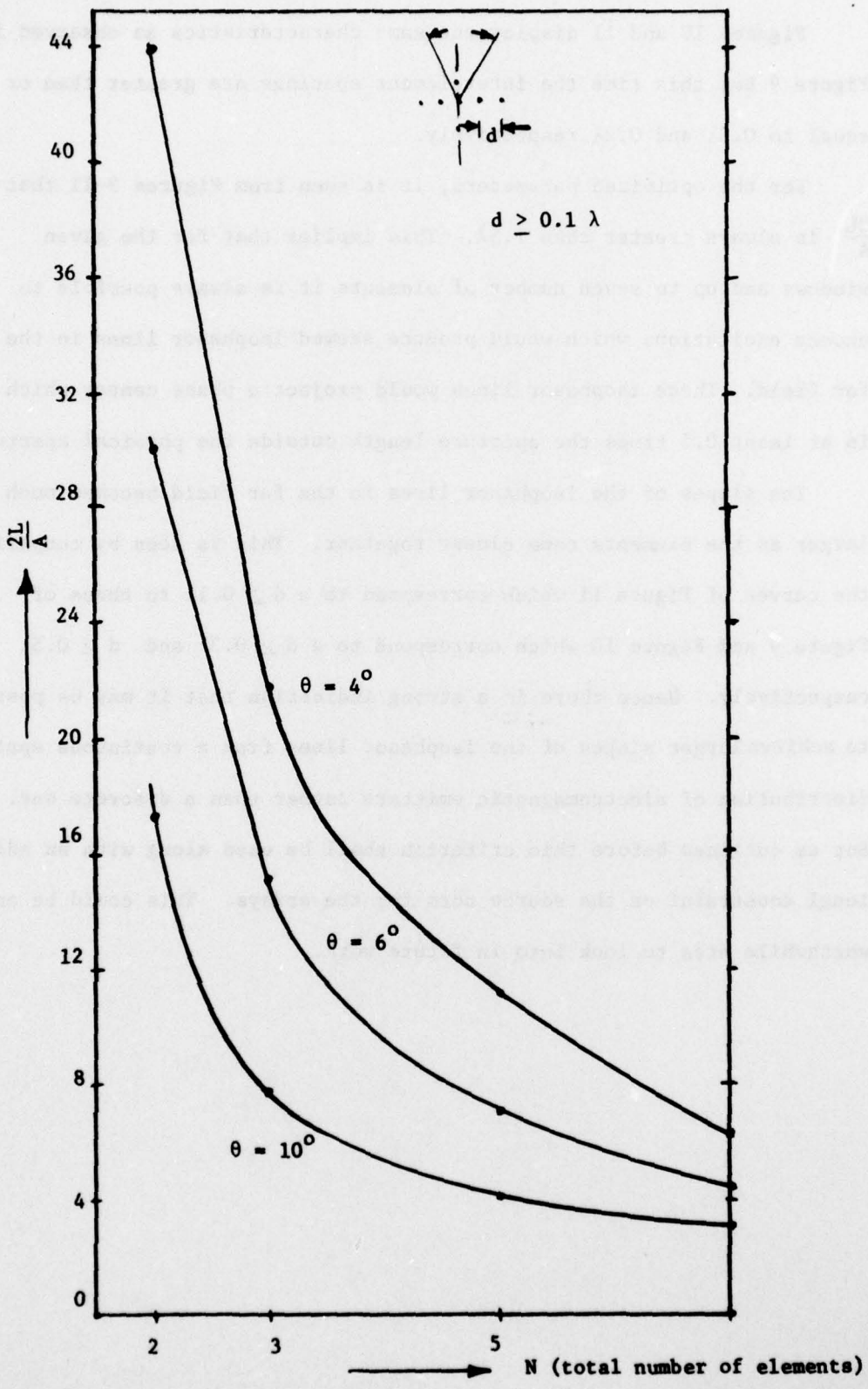

Figure 11: 2L/A for various elements having 0.1 λ as an interelement spacing

Figures 10 and 11 display the same characteristics as observed in Figure 9 but this time the interelement spacings are greater than or equal to 0.3λ and 0.2λ respectively.

For the optimized parameters, it is seen from Figures 9-11 that $\frac{2L}{A}$ is always greater than 1.5λ. This implies that for the given windows and up to seven number of elements it is always possible to choose excitations which would produce skewed isophasor lines in the far field. These isophasor lines would project a phase center which is at least 0.5 times the aperture length outside the physical aperture.

The slopes of the isophasor lines in the far field becomes much larger as the elements come closer together. This is seen by comparing the curves of Figure 11 which correspond to a $d \geq 0.1\lambda$ to those of Figure 9 and Figure 10 which correspond to a $d \geq 0.3\lambda$ and $d \geq 0.5\lambda$ respectively. Hence there is a strong indication that it may be possible to achieve larger slopes of the isophasor lines from a continuous spatial distribution of electromagnetic emitters rather than a discrete one. But as outlined before this criterion shall be used along with an additional constraint on the source norm for the arrays. This could be an worthwhile area to look into in future work.

V. CONCLUSION

The possibility of obtaining skewed isophasor lines from two emitters has been illustrated by Meade [1] and Howard [2]. From their results it is seen that large slopes of the isophasor lines could only be achieved over a narrow window. The theory developed in this report could be applied to obtain skewed isophasor lines over large angle windows. Also of importance is the fact that sometimes the power density is considerably greater than that indicated by Meade [1] and Howard [2].

The theory presented in this report can also be applied to time waveforms where the apparent time of arrival of the waveform can be changed with appropriate phasing of the electromagnetic emitters. Another important application is in the guidance of a missile by the skewed isophasor lines. It may also be applied in the case of Displaced Phase Center Antenna (DPCA) to counteract the linear motion of the airborne radar. However the technique presented here can find applications to many other electronic systems.

REFERENCES

1. J.E. Meade, "Target Considerations," in A.S. Locke, et. al., "Guidance," D. VanNostrand Co., Inc., Princeton, N.J., ch. 11, 1955.

2. D.D. Howard, "Radar Target Angular Scintillation In Tracking And Guidance Systems Based On Echo Signal Phase Front Distortion," Proceedings of National Electronics Conference, Vol. 15, pp. 840-849, 1959.

3. F.I. Tseng and D.K. Cheng, "Transient and Steady-State Antenna Pattern Characteristics for Arbitrary Time Signals," Technical Report RADC-TR-66-101, June 1965. (484512)

4. H.H. Rosenbrock, "An Automatic Method for Finding the Greatest or Least Value of a Function," "The Computer Journal," Vol. 3, pp. 175-184.

APPENDIX A - ROSENBROCK'S OPTIMIZATION METHOD

The function - minimization algorithm due to Rosenbrock [4] is well known but is included here for completeness.

The Rosenbrock search technique uses M mutually orthogonal directions during each search cycle to find a relative minimum. This strategy differs from a steepest descent technique which uses successive orthogonal directions, but these successive directions do not necessarily form a mutually orthogonal set. The M mutually orthogonal directions are the basis for the success of this technique. Moreover, unlike the other optimum search procedures this method does not require any derivatives of the functions to be minimized. The basic elements of the Rosenbrock algorithm are as follows:

a) Step Size: The step size in a given direction is chosen by specifying an arbitrary magnitude h and then, if a step h decreases the value of the function (for a minimization problem), h is multiplied by a constant ($\alpha>1$). If the value of the function increases, h is multiplied by a constant - $\beta(0< \beta < 1)$. h should be on the order of one percent of the average magnitude of the variables. To determine the values of α and β, a series of trials using various values of α and β should be made for a given class of functions for which the function to be minimized belongs.

b) Direction: The Rosenbrock algorithm uses M mutually orthogonal directions $d_1, d_2, \ldots, d_M$ at each stage rather than choosing a single direction in which to progress. Therefore, a search is made in each orthogonal direction before the next step is chosen (at least, one trial has been successful - a value less than or equal to the old value - and one has failed in each direction).

There are three cases to consider:

i) The first trial is a success.

ii) The first trial is a failure and the second trial is a success.

iii) The first trial is a failure and the second trial is a failure.

For a start, let $[D^0] = [U]$ (identity matrix) where $d_1^0, d_2^0, \ldots, d_M^0$ are individual directions in which steps are to be taken. The search technique progresses as follows (for one variable x_1):

1) A step is taken in the direction d^0 from an initial point x^0

$$x^1 = h\ (x^0 \cdot d_1^0).$$

2) If $f\ (x^1) < f\ (x^0)$, the step is successful and the step size is multiplied by α again and again until a failure is recorded. After this failure, the result of the last succcessful trial and the number of successful trials is stored.

3) If $f\ (x^1) > f\ (x^0)$ on the first trial, a failure results and the sign of the step size h is changed and the search continues as in (2).

4) If $f\ (x^1) > f\ (x^0)$ and $f\ (x^2) > f\ (x^0)$, the second and further trials are determined by multiplying h by minus β until a success is recorded. After a search has been made for each variable in all directions d_1^0, a new $[D^1]$ is determined. Let g_i be the algebric sum of all the successful steps h_i in the direction d_i^0. Then the first element d_1^1 of $[D^1]$ is chosen as the vector sum of all the vectors $\sum_i g_i d_i^0$. The other elements of $[D^1]$ are determined using the Gram-Schmidt orthogonalization procedure. Let

$$\begin{aligned} A_1 &= g_1 d_1^0 + g_2 d_2^0 + \ldots + g_M d_M^0 \\ A_2 &= \quad g_2 d_2^0 + \ldots + g_M d_M^0 \\ &\vdots \\ A_M &= \quad g_M d_M^0 \end{aligned}$$

where A_1 is the vector joining the initial and final points obtained by the sum of vectors d_i^0, and A_2 is the sum of the successes achieved in the directions

other than the first and so on. Then from the Gram-Schmidt orthogonalization procedure

$$B_1 = A_1$$

$$d_1^1 = \frac{B_1}{|B_1|}$$

$$B_2 = A_2 - (A_2{}^T \cdot d_1^1)\, d_1^1 \qquad \text{where T is the transpose}$$

$$d_2^1 = \frac{B_2}{|B_2|}$$

$$\vdots$$

$$B_M = A_M - \sum_{m=1}^{M-1} (A_M^T \cdot d_m^1)\, d_m^1$$

$$d_M^1 = \frac{B_M}{|B_M|}$$

So for the second iteration the searches are made in M orthogonal directions of $[D^1]$. The process is continued until a convergence criterion is satisfied. The computer program listing for this procedure is listed below.

```
1070 SUBROUTINE ROTATE(X,N,VF,U,H,VV,NFIRST)
1080 dimension d(39),x(30),u(30,30),a(30,30),b(30),un(30,30),ns(40)
1090 bb=0.5
1100 aa=3.0
1110 if(nfirst-1) 15,15,17
1120 15 do 24 i=1,n
1130 d(i)=0.0
1140 do 25 j=1,n
1150 25 u(i,j)=0.0
1160 24 u(i,i)=1.0
1170 vv=vf(x)
1180 17 do 1 j=1,n
1190 ns(j)=0
```

```
1200 l=1
1210 e=h
1220 vvt=vv
1230 2 do 3 i=1,n
1240 3 b(i)=x(i)+e*u(j,i)
1250 dv=vf(b)-vv
1260 vv=vv+dv
1270 go to (4,5,26,27),l
1280 4 l=3
1290 if(dv) 28,28,29
1300 29 l=2
1310 vv=vv-dv
1320 e=-h
1330 go to 2
1340 5 l=3
1350 if(dv) 28,28,35
1360 35  l=4
1370 41 if(ns(j)+20) 44,44,47
1380 47 e=-bb*e
1390 ns(j)=ns(j)-1
1400 go to 2
1410 28 e=aa*e
1420 ns(j)=ns(j)+1
1430 go to 2
1440 26 if(dv) 28,28,42
1450 42 e=e/aa
1460 vv=vv-dv
1470 go to 44
1480 27  dv=vvt-vv
1490 if(dv)41,41,44
1500 44 do 45 i=1,n
1510 45 x(i)=x(i)+e*u(j,i)
1520 1 d(j)=e
1530 do 9 m=1,n
1540 c=0.0
1550 do 6 i=1,n
1560 zz=0.0
1570 do 7 j=m,n
1580 7 zz=zz+d(j)*u(j,i)
1590 if (m-1) 32,32,8
1600 8  mm=m-1
1610 do 11 j=1,mm
1620 z=0.
1630 do 12 k=1,n
1640 v=0.
1650 do 13 l=m,n
1660  13 v=v+d(l)*u(l,k)
1670 12 z=z+v*un(j,k)
1680 a(m,j)=z
1690 11 continue
```

```
1700 do 14 j=1,mm
1710 14 zz=zz-a(m,j)*un(j,i)
1720 32 b(i)=zz
1730 6 c=c+zz*zz
1740 c=1./sqrt(c)
1750 do 10 i=1,n
1760 10 un(m,i)=c*b(i)
1770 9 continue
1780 do 18 i=1,n
1790 b(i)=0.0
1800 do 19 j=1,n
1810 19 u(i,j)=un(i,j)
1820 18 continue
1830 return
1840 end
```

APPENDIX B - COMPUTER PROGRAM DESCRIPTION

The user-oriented computer program consists of a main program which supplies all the necessary data required for the execution of the computer program and subprograms. The first subprogram FUN in this case, defines the function to be minimized and the second subprogram ROTATE is the optimization method due to Rosenbrock. The latter is described in Appendix A.

The main program supplies all the input data. The input data consist of the following statements. Statement number 40 provides the value for N (as shown in Fig. 1) through MNE.

Statement numbers 90-120 provide the initial guess for the excitations of the electromagnetic emitters in the first N8 elements of the array Y. The elements of Y(I) are defined in the following manner:

$$a_1 = 0.5\,[Y(1) + Y(2)]$$

$$b_1 = 0.5\,[Y(3) + Y(4)]$$

$$a_{-1} = 0.5\,[Y(2) + Y(1)]$$

$$b_{-1} = 0.5\,[Y(3) - Y(4)]$$

and so on. The statement number 130 provides the initial guess for the inter-emitter spacing for the array through Y(N9).

Statement number 150 defines the value of $\frac{2L}{A}$ through the constant SLOPE.

Statement numbers 170-180 define the angle window over which the desired slope is to be achieved. MP provides the start of the angle window in degrees and MQ is the last angle of the window, taken at steps

of MR degrees. It is not necessary to have the window symmetrically placed around the z-axis of Fig. 1.

Statement number 250 specifies the maximum number of iterations to be made by the optimization method to yield the final result.

Statements 390, 400 and 480 provide the excitations for the array elements and 490 prints the value for the interelement spacing and the value of the function through VFVAL at the end of each iteration.

580 prints the slope, the magnitude and phase for the far field within the specified window. This is done at the end of the final iteration.

Statement 650 defines the constraint imposed on the inter-element spacing. For this problem interelement spacing cannot be less than or equal to 0.4λ.

The program as presented represents a 3 element array for MNE=1. So for a 2-element array the necessary modifications of the program are as follows. The statements 450-490, 870-880 should be deleted. Statement 80 should read N9 = N7. Statement 641 should be introduced to read N9 = N7. In statement 650, the contraint should be changed to half the interelement spacing desired. For example, if the problem be such that the interelement spacing for a 2 element array be restricted to be greater than or equal to 0.5λ then $Y(N9) \geq 0.25$.

The computer program listing is presented below.

```
10 EXTERNAL FUN
20 COMMON /AJ/MP,MQ,MR,MS,SLOPE,MNE,N7,N8,N9,CC
30 DIMENSION Y(30),AXES(30,30)
40 MNE=3
50 N6=4*MNE
60 N7=N6+1
70 N8=N7+1
80 N9=N8+1
90 Y(1)=1.0
100 Y(2)=0.01
```

```
      DO 11 I=3,N8
   11 Y(I)=0.
      Y(N9)=0.7
      H=0.01
      SLOPE=16
      PP=180./3.14159263
      MP=177
      MQ=183
      MR=1
      MS=0
      J=1
      NQ=N9
      PRINT 189,MNE,MP,MQ,SLOPE,Y(N9)
  189 FORMAT('0 ',3I9,2F10.5)
      DO 2 II=1,10
      CALL ROTATE (Y,NQ,FUN,AXES,H,VFVAL,J)
      NN=1
      CC=0
      DO 23 NL=1,MNE
      A1=0.5*(Y(NN)+Y(NN+1))
      B1=0.5*(Y(NN+2)+Y(NN+3))
      A2=0.5*(Y(NN+1)-Y(NN))
      B2=0.5*(Y(NN+2)-Y(NN+3))
      C1=SQRT(A1*A1+B1*B1)
      C2=SQRT(A2*A2+B2*B2)
      D1=PP*ATAN2(B1,A1)
      D2=PP*ATAN2(B2,A2)
      CC=CC+C1*C1+C2*C2
      PRINT 108,NL,A1,B1,C1,D1
      PRINT 108,-NL,A2,B2,C2,D2
  108 FORMAT(' ',I5,4F15.5)
      NN=NN+4
   23 CONTINUE
      NL=0
      C1=SQRT(Y(N7)*Y(N7)+Y(N8)*Y(N8))
      D1=PP*ATAN2(Y(N8),Y(N7))
      CC=SQRT(CC+C1*C1)
      PRINT 108,NL,Y(N7),Y(N8),C1,D1
      PRINT 100,Y(N9),VFVAL
      IF(VFVAL.EQ.0.) GO TO 5
  100 FORMAT(' ',4F15.7)
      J=J+1
    2 CONTINUE
    5 MS=1
      MP=MP-3
      MQ=MQ+3
      MR=1
      ZZ=FUN(Y)
    6 CONTINUE
      STOP
      END
```

```
      FUNCTION   FUN(Y)
      DIMENSION Y(30)
      COMMON /AJ/MP,MQ,MR,MS,SLOPE,MNE,N7,N8,N9,CC
      IF(Y(N9).LE.0.4) GO TO 4
      DO 12 I=1,N9
   12 IF(ABS(Y(I)).GT.10.)GO TO 4
      FUN=0.
      DO 1 I=MP,MQ,MR
      PI=0.0174533*FLOAT(I)
      PHI=6.283186*SIN(PI)*Y(N9)
      UP=0.0
      DN=0.0
      NN=1
      U1=0.
      U3=0.
      DO 2 N=1,MNE
      THT=N*PHI
      CT=COS(THT)
      ST=SIN(THT)
      UP=UP+Y(NN)*ST+Y(NN+2)*CT
      DN=DN+Y(NN+1)*CT-Y(NN+3)*ST
      U1=U1+N*(Y(NN)*CT-Y(NN+2)*ST)
      U3=U3+N*(Y(NN+1)*ST+Y(NN+3)*CT)
      NN=NN+4
    2 CONTINUE
      UP=UP+Y(N8)
      DN=DN+Y(N7)
      SP=COS(PI)*(U1*DN+U3*UP)/(UP*UP+DN*DN)
      SP=SP/FLOAT(MNE)
      IF (MS.EQ.1) GO TO 11
      SP=ABS(SP)
      IF(SP.LT.SLOPE) FUN=FUN+SLOPE-SP
      GO TO 1
   11  AAG=SQRT(UP*UP+DN*DN)
      AAG=AAG/CC
      AAG=20.*ALOG10(AAG)
      SR=ATAN2(UP,DN)
      SI=180./3.14159263*SR
      PRINT 101,I,AAG,SI,SP
  101 FORMAT(' ',I5,3F15.3)
    1 CONTINUE
      RETURN
    4 FUN=100.
      RETURN
      END
```

APPENDIX C - COMPLEX EXCITATIONS OF THE OPTIMIZED ARRAY

The complex excitations of the electromagnetic emitters that yield a prescribed slope of the phase of the far-field pattern are presented in this section.

The complex excitations required to yield the far-field pattern presented in Figure 4 are as follows:

$$a_1 = 0.087 \quad \angle 12.20^\circ$$

$$a_{-1} = 0.034 \quad \angle 4.96^\circ$$

$$a_0 = 0.093 \quad \angle -171.34^\circ$$

Similarly for the field pattern for the 2 element array presented in Figure 5, the excitations are as follows:

$$a_1 = 0.165 \quad \angle 8.37^\circ$$

$$a_{-1} = 0.062 \quad \angle -171.63^\circ$$

For Figure 7, the excitations are:

$$a_1 = .111 \quad \angle 2.52^\circ$$

$$a_{-1} = 0.069 \quad \angle 177.91^\circ$$

$$a_0 = 0.014 \quad \angle 164.35^\circ$$

The corresponding excitations for Figure 8 are:

$$a_1 = 0.132 \quad \angle 0.29^\circ$$

$$a_{-1} = 0.095 \quad \angle 178.92^\circ$$

Finally the complex excitations required for a 7 element array to yield point B in Figure 9 are as follows:

$$a_1 = 0.096 \angle 6.95^\circ$$

$$a_{-1} = 0.082 \angle -175.34^\circ$$

$$a_2 = 0.043 \angle -164.99^\circ$$

$$a_{-2} = 0.045 \angle -5.58^\circ$$

$$a_3 = 0.017 \angle -84.82^\circ$$

$$a_{-3} = 0.004 \angle -72.45^\circ$$

$$a_0 = 0.032 \angle 124.42^\circ$$